

Cross- α / β Polymorphism of PSM α 3 Fibrils

Olivia M. Cracchiolo^{[a], [+]}, Dean N. Edun^{[a], [+]}, Vincent M. Betti^[b], Jacob M. Goldberg^[b], and Arnaldo L. Serrano^{*[a]}

[a] [*] Olivia M. Cracchiolo, Dean N. Edun, and Arnaldo L. Serrano
Department of Chemistry and Biochemistry
University of Notre Dame
251 Nieuwland Science Hall,
Notre Dame, IN 46556
E-mail: arnaldo.serrano@nd.edu

[b] Vincent M. Betti and Jacob M. Goldberg
Department of Chemistry
Colgate University
13 Oak Drive,
Hamilton, NY 13346
Email: jgoldberg@colgate.edu

[+] These authors contributed equally to this work

Supporting information for this article is given via a link at the end of the document.

Abstract: The formation of ordered cross- β amyloid protein aggregates is associated with a variety of human disorders. While conventional infrared methods serve as sensitive reporters of the presence of these amyloids, the recently discovered amyloid secondary structure of cross- α fibrils presents new questions and challenges. Herein, we report results using Fourier Transform infrared (FTIR) spectroscopy and two-dimensional infrared (2DIR) spectroscopy, to monitor the aggregation of one such cross- α forming peptide, phenol soluble modulins alpha 3 (PSM α 3). Phenol soluble modulins (PSMs) are involved in the formation and stabilization of *Staphylococcus aureus* biofilms, making sensitive methods of detecting and characterizing these fibrils a pressing need. Our experimental data, coupled with spectroscopic simulations, reveals the simultaneous presence of cross- α and cross- β polymorphs within samples of PSM α 3 fibrils. We also report a new spectroscopic feature indicative of cross- α fibrils.

Amyloids are elongated fibers of proteins or peptides, typically composed of stacked cross β -sheets.^[1,2] Self-assembling amyloids are notorious for their involvement in human neurodegenerative diseases such as Alzheimer's and Parkinson's diseases.^[1,2] Phenol soluble modulins (PSMs) are amyloid peptides secreted by the bacteria *Staphylococcus aureus* (*S. aureus*).^[3-5] Of the PSM family, PSM α 3, is of recent interest due to its unique secondary structure upon fibrillation. Whereas other PSM variants undergo conformational changes with aggregation, the α -helical PSM α 3 peptide retains its secondary structure while stacking in a manner reminiscent of β -sheets, forming what has been termed cross- α fibrils.^[3,4,6] Although, " α -sheet" amyloid fibrils have been previously observed in 2DIR^[7] and associated with PSMs,^[8] the novel cross- α fibril is distinct from that class of structures. Interestingly, shorter terminations of PSM α 3 have been shown to exhibit β -sheet polymorphs.^[9] The proposed cross- α fibril structure of the full length PSM α 3 peptide has been confirmed with x-ray diffraction (XRD), and circular dichroism

(CD).^[4] The present study aims to further characterize these fibrils with linear and non-linear infrared spectroscopies (see Supplementary Information (SI) for experimental details).

S. aureus is an infectious human pathogen with the ability to form communities of microorganisms called biofilms that hinder traditional treatment methods.^[10-12] PSMs contribute to inflammatory response and play a crucial role in structuring and detaching biofilms.^[9-11] While biofilm growth requires the presence of multiple PSMs,^[10,13] Andreassen and Zaman have demonstrated that PSM α 3 acts as a scaffold, seeding amyloid formation of other PSMs.^[5] To effectively inhibit *S. aureus* biofilm growth, a better understanding of PSM α 3 aggregation is needed.

The α -helical structure of PSM α 3^[11] presents a challenge for probing the vibrational modes and secondary structure of both the monomer and the fibrils. While IR spectroscopy has been used extensively to characterize β -sheets,^[14-17] the spectral features associated with α -helices are difficult to distinguish from those of the random coil secondary structure.^[18,19] This limitation has left researchers to date with an incomplete picture of the spectroscopic features unique to cross- α fibers. The present work combines a variety of 2DIR methods to remove these barriers and probe the active infrared vibrational modes of cross- α fibers.

The full length 22-residue, PSM α 3 peptide was synthesized (see SI for details) and prepared for aggregation studies following reported methods.^[3,4,9] 10 mM PSM α 3 was incubated in D₂O at room temperature over 7 days. These data were compared to the monomer treated under similar conditions. Monomeric samples were prepared at a significantly lower concentration of 0.5 mM to prevent aggregation. Fiber formation was confirmed by Transmission Electron Microscopy (TEM, see Figure S1 Supporting Information for details). FTIR spectra were taken for both the fibrils in solution as well as the low concentration monomers. Spectroscopic simulations of the PSM α 3 monomer and fibers were performed on previously reported PDB structures^[11] (Figure 1).

In general, IR spectra of monomeric α -helices can typically be characterized by 3 nearly degenerate modes, the A mode, and the doubly degenerate E modes, appearing as a broad peak centered at 1650 cm^{-1} .^[16,18,20] Comparing the FTIR spectrum (Figure 1c) of the low concentration monomer (blue) with that of the fibrils in solution (red), reveals a broad peak centered around 1650 cm^{-1} in both spectra, with no significant spectroscopic differences. This broad peak is indicative of either an α -helical or random coil secondary structure.^[21] FTIR alone is unable to distinguish between the two structures or resolve any conformational changes between the two samples. To address these ambiguities, we turned to the versatile technique of two-dimensional infrared (2DIR) spectroscopy. 2DIR has been widely used in studies of protein folding^[22,23] and amyloid aggregation^[17,24] due to its sensitivity to secondary structure.^[25,26] Similar to 2D NMR, 2DIR is a correlation spectroscopy that reports on vibrationally coupled modes via the emergence of cross peaks.^[27] In efforts to isolate cross peaks, different combinations of the pump and probe beam polarizations may be employed. The present study employs polarization dependent 2DIR using a combination of broad band (BB) and narrow band (NB) pump experiments in order to isolate cross peaks characteristic of secondary and tertiary structure.^[17,28]

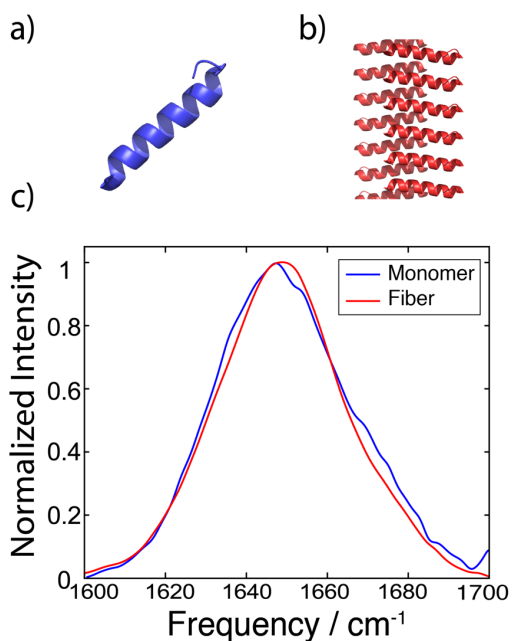


Figure 1. PDB structures of PSM α 3 monomers a) and fibers b) extended along the screw-axis. c) FTIR spectra of 0.5 mM monomeric PSM α 3 (blue) compared to the 10 mM PSM α 3 fibril (red) in D₂O upon aggregation

A 2DIR spectrum stretches the linear spectrum over two axes with each peak in the FTIR appearing as a peak pair. The positive peak (red) corresponds to the ground state bleach and stimulated emission (the 0-1 vibrational transition), while the negative peak (blue) corresponds to the excited state absorption (the 1-2 transition). To investigate potential conformational changes during the fibrillation process, a weeklong incubation was monitored with 2DIR (Figure 2), using an 8-frame phase cycling scheme, as described below. The 2DIR spectrum in Figure 2a has one spectral feature centered around 1650 cm^{-1} (probe) at 25 minutes into the incubation. This peak position is consistent with

the initial α -helical structure of the monomer observed in the FTIR spectrum. No significant spectral changes were observed until day four (Figure 2c), when a second peak pair emerged at 1622 cm^{-1} (probe). This spectral region is predominantly characteristic of β -sheets.^[16,21,27] β -sheets have a defining set of cross peaks making them easy to distinguish from other spectral features in this region.^[14,29] To definitively assign this peak pair at 1622 cm^{-1} to β -sheets we relied on polarization dependent spectra, which will be discussed below. By the seventh day (Figure 2d) no further spectral changes were observed.

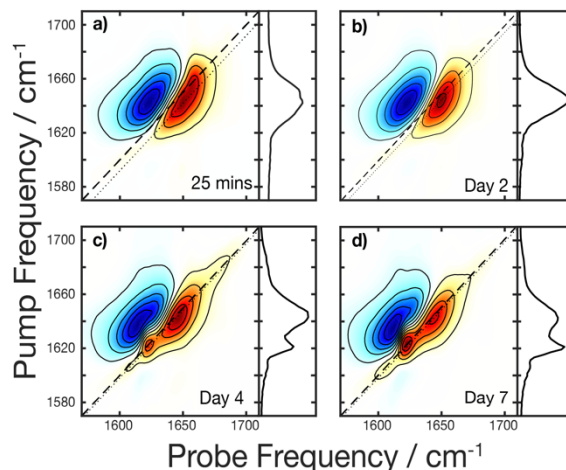


Figure 2. 2DIR spectra monitoring the weeklong aggregation of 10 mM PSM α 3 in D₂O taken at the time points indicated in the lower right corner. The dotted lines correspond to the diagonal slices shown in the panels to the right of each spectrum.

It is important to note that while the signal in an FTIR spectrum scales as μ^2 (the transition dipole moment squared), 2DIR signals scale as μ^4 , leading to signal enhancement for highly coupled systems, such as the protein backbone of a β -sheet.^[24,25,30,31] Therefore, it is not surprising that despite the strong intensity of the 1622 cm^{-1} peak in the 2DIR spectrum, this peak is not readily apparent in the FTIR data. A recent study estimated that 20% - 40% of PSM α 3 fibrils adopt a β -sheet population. These investigators have also shown that short regions within PSM α 3 act as seeds for amyloid β -aggregation.^[5] In the spectrum, a peak remains at 1649 cm^{-1} after incubation. To determine whether this peak originates from cross- α fibrils or solubilized monomers, we turned to phase cycling.

We used phase cycling to measure the relative amplitude of pump-light scattered by the sample region being studied, as fibers are strong light scatterers.^[32] In practice, our measured data are proportional to the absolute value squared of the sum of all complex valued electric field contributions as shown in equation 1, where E_1 and E_2 are the pump fields, s is a scattering amplitude, E_{LO} is the local oscillator field (which is also the probe in our experiment),^[33] and E_{sig} is the emitted 2DIR signal field.

$$I \propto |sE_1 + sE_2 + E_{LO} + E_{sig}|^2 = (|E|^2 \text{ terms}) + |s|^2 E_1^* E_2 + s^* E_1^* E_{LO} + s^* E_1^* E_{sig} + s^* E_2^* E_{LO} + s^* E_2^* E_{sig} + E_{LO}^* E_{sig} + c. c. \quad (1)$$

Equation 1 focuses on the cross terms, which are what primarily contribute to or contaminate the 2D spectrum. The heterodyned 2DIR signal, $E_{LO}^*E_{sig}$, is processed to produce 2D spectra, while $(s^*E_1^*E_{sig} + s^*E_2^*E_{sig})$ are the smallest terms and can be neglected. The remaining terms require phase cycling to remove.^[17,34,35] Using a pulse shaper-based spectrometer permits shot-to-shot control of the phases of the two pump pulses. By carefully selecting phases and combining measurements, particular signals can be cancelled, which is highly effective at removing these scattered light signals. A typical 4-frame phase cycling scheme is presented in equation 2, where $I_{[\phi_1, \phi_2]}$ represents data where the phases for the first and second pump pulses are set to ϕ_1 and ϕ_2 , respectively.

$$S_{2D} \propto (I_{[0,0]} + I_{[\pi,\pi]}) - (I_{[0,\pi]} + I_{[\pi,0]}) \quad (2)$$

By combining the phase cycled measurements in this manner, the terms in equation 1 linear in s cancel out entirely. Normally, scattered light is a nuisance to obtaining clean spectra. However, in order to isolate the signal from fibrils, areas with intense light scattering were chosen. To do this, we used the scattered light contamination described above to our advantage by combining the phase cycled measurements according to equation (3). This scheme cancels the 2DIR signal while enhancing $s^*E_1^*E_{LO}$.

$$S_{scat} \propto (I_{[0,0]} + I_{[0,\pi]}) - (I_{[\pi,0]} + I_{[\pi,\pi]}) \quad (3)$$

Using S_{scat} we were able to identify sample regions with both large 2DIR signal and large scattering amplitudes (see Figure S2), which we assign to fibrillar samples and from which data in Figures 3 and 4 were collected. Within the conventional 4-frame phase cycling scheme in equation 2, the pump-pump cross term will survive, which, though often neglected due to its $|s|^2$ scaling, is problematic for measuring 2DIR of particularly strong scatterers such as solids. To measure signals associated with fibrils and remove this source of scattering, we employed an 8-frame phase cycling scheme that eliminates this term.^[36,37] In the 8-frame scheme, we used an optical chopper to chop the probe pulse every second laser shot. The 8 frames are combined according to equation (4), where ON and OFF refer to the probe beam. This 8-frame scheme is employed in all 2DIR spectra following the initiation of aggregation (Figure 2a).

$$S_{2D} \propto \left\{ (I_{[0,0,ON]} + I_{[\pi,\pi,ON]}) - (I_{[0,\pi,ON]} + I_{[\pi,0,ON]}) \right\} - \left\{ (I_{[0,0,OFF]} + I_{[\pi,\pi,OFF]}) - (I_{[0,\pi,OFF]} + I_{[\pi,0,OFF]}) \right\} \quad (4)$$

We performed broad band (BB) 2DIR experiments with 8-frame phase cycling using both parallel (Figure 3a) and perpendicular (Figure 3b) polarizations on a 1-week incubated sample at a spot with high scattering (Figure S2b). These spectra show peaks in both the α /random-coil and β dominant spectral regions (1650 and 1620 cm^{-1} , respectively). Figure 3c shows a difference spectrum between the normalized parallel and perpendicular spectra. In a difference spectrum, the diagonal peaks are suppressed, enhancing the cross peak signals^[38,39]. The BB difference spectrum (Figure 3c) reveals a potential set of cross peaks (denoted B') at (probe, pump) = (1689, 1622) cm^{-1} , however the signal for its matching peak pair, which should appear in the region denote B, is weak and difficult to resolve. In addition, there remain peaks along the diagonal.

A BB measurement simultaneously excites all modes within the spectral bandwidth. This leads to the so-called "diagonal" cross peaks that are prevalent in Figure 3c.^[39] An effective strategy to remove these coherent signals and isolate the off-diagonal cross peak signal is to preferentially excite one mode at a time, which can be achieved by switching to a narrow band pump (NB) 2D measurement,^[28,40] though the signal is inherently noisier with this technique.^[39,41] The NB difference spectrum (Figure 3f) reveals cross peak pairs at (probe, pump) = (1620, 1687) cm^{-1} and (1682, 1623) cm^{-1} (denoted B and B' respectively), consistent with previously reported β -sheets.^[42] We also observe characteristic α -helical cross peak pairs at (probe, pump) = (1653, 1662) and (1663, 1645) cm^{-1} , denoted A and A'.^[22,23,43] The peaks in these regions arise from coupling between the A and E modes. Random coil peptides would not give rise to any cross peaks,^[19] hence we can confidently assign the 1650 cm^{-1} peak to α -helices.

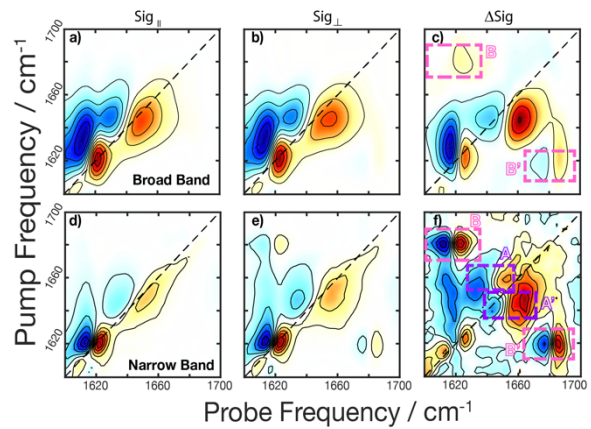


Figure 3. 2DIR spectra of aggregated PSM α 3 taken with parallel (column 1) and perpendicular (column 2) polarizations using broad band pump (a-c) and narrow band pump (d-f) pulses taken at the same sample position. The difference spectra are shown in the last column with the dashed boxed highlighting cross peak regions for α -helices (purple) denoted A and A', and β -sheets (pink) denoted B and B'.

In order to isolate spectral features of purely cross- α fibrils, the BB (Figure 4a-c) and NB (Figure 4d-e) pump experiments were repeated at a new location in the sample where only α -helical peaks (1650 cm^{-1}) were present, along with scattered light indicating the presence of fibrils (Figure S2c). Once again, a strong coherent signal appeared along the diagonal of the BB polarization difference spectrum (Figure 4c), while the NB difference spectrum (Figure 4f) revealed α -helical cross peaks (A and A') at (probe, pump) = (1661, 1648) cm^{-1} and (1651, 1662) cm^{-1} matching those in Figure 3f. The coherent signal along the diagonal of the BB polarization difference spectrum (Figure 4c) has the structure of a non-rephasing lineshape, which is consistent with a diagonal cross-peak between two strongly coupled states

To ensure this spectroscopic signal is unique to cross- α fibrils, and not inherent to monomeric PSM α 3, the BB experiments were repeated with a monomeric sample (Figure S3). The monomer BB difference spectrum does not reveal the same coherent cross peak pattern as the fibril, but rather shows peaks similar to those denoted A and A' in Figures 3f and 4f. Therefore, we assign the peak pattern in Figure 4c to a diagonal coherent cross peak

between modes within the stacked cross- α fibril. The stacked structure allows for new combinations of A and E mode interactions that would not be possible in the monomeric α -helix alone, suggesting that this signal can serve as a probe of cross- α formation.

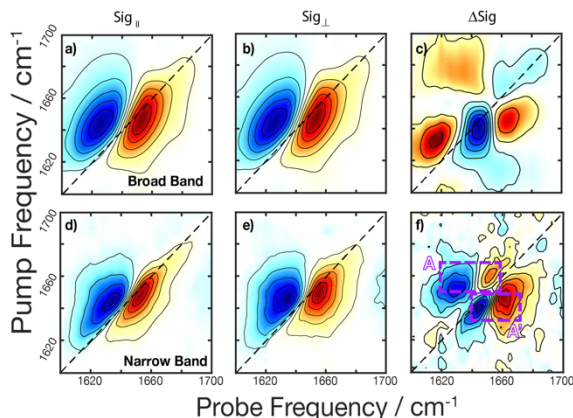


Figure 4. 2DIR spectra of PSM α 3 cross- α fibrils taken with parallel (column 1) and perpendicular (column 2) polarizations using broad band pump (a-c) and narrow band pump (d-f) pulses taken at the same sample position. The difference spectra are shown in the last column with the dashed boxed highlighting cross peak regions for the α -helix (purple) denoted A and A'.

In order to validate the assignments of the experimental spectra, 2DIR simulations were performed. Due to the extended nature of the system, it was necessary to simulate a 40 unit cell long system, which corresponded to 1760 interacting peptide units. Because conventional sum over state 2DIR simulations protocols would be unfeasible on such a large system, we opted to use the Nonlinear Exciton scattering approach of Mukamej^[44–49] (see SI for details). The parallel and perpendicular BB 2D spectra were simulated for the 40-unit fibril of PSM α 3, and the difference spectrum is plotted in Figure 5b. The simulated BB difference spectrum (Figure 5b) possesses a strong peak with a non-rephasing lineshape along the diagonal, similar to what was observed experimentally (Figure 5a). In addition, simulation of monomeric peptide prior to aggregation are also consistent with experiment (Figure S4). Therefore, this peak pattern in the polarization difference spectrum can be used to infer the presence of cross- α fibrils.

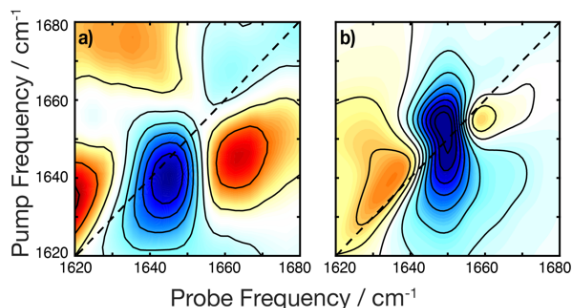


Figure 5. 2DIR broad band pump difference spectra of PSM α 3 cross- α fibrils a) experimental b) simulated spectrum of a 40-unit fibril.

While identifying this peak required collection of multiple spectra, some versions of the 2DIR experiment can directly access the

information in the polarization difference spectrum in a single measurement.^[39]

In conclusion, the 22-residue peptide, PSM α 3 was shown to exhibit cross- α and cross- β polymorphism at room temperature within the same samples. Structural polymorphism, in the sense of different structures being observed under different aggregation conditions, has been observed in the past for PSM peptides,^[4,9] but to our knowledge this is the first evidence of α/β polymorphs existing in equilibrium with each other. We also present a spectroscopic signature, resulting from coherent cross peaks in the 2DIR data, that uniquely reports on cross- α fibril secondary structure. Further study is required to identify the specific spectroscopic pathways giving rise to this coherent cross peak.

Acknowledgements

ALS gratefully acknowledges support from the College of Science at the University of Notre Dame. We thank Dr. Mijoon Lee in the Mass Spectrometry and Proteomics Facility at University of Notre Dame and Dr. Maksym Zhukovskiy in the Integrated Imaging Facility at University of Notre Dame.

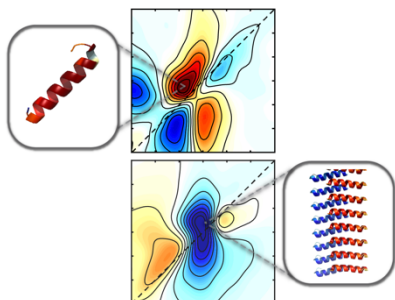
Keywords: cross- α fibrils • coherent cross peaks • polymorphism • 2DIR • PSM α 3 • amyloid

- [1] D. Eisenberg, M. Jucker, *Cell* **2012**, *148*, 1188–1203.
- [2] M. R. Nilsson, *Methods* **2004**, *34*, 151–160.
- [3] E. Tayeb-Fligelman, O. Tabachnikov, A. Moshe, O. Goldshmidt-Tran, M. R. Sawaya, N. Coquelle, J. P. Colletier, M. Landau, *Science* (80). **2017**, *355*, 831–833.
- [4] E. Tayeb-Fligelman, N. Salinas, O. Tabachnikov, M. Landau, *Structure* **2020**, *28*, 301-313.e6.
- [5] M. Zaman, M. Andreasen, *Elife* **2020**, *9*, 1–17.
- [6] M. Das, S. Dash, B. L. Bhargava, *Chem. Phys.* **2020**, *535*, 1–9.
- [7] M. R. Hilaire, B. Ding, D. Mukherjee, J. Chen, F. Gai, *J. Am. Chem. Soc.* **2018**, *140*, 629–635.
- [8] A. Bleem, R. Francisco, J. D. Bryers, V. Daggett, *npj Biofilms Microbiomes* **2017**, *3*, DOI 10.1038/s41522-017-0025-2.
- [9] N. Salinas, J. P. Colletier, A. Moshe, M. Landau, *Nat. Commun.* **2018**, *9*, 3512.
- [10] S. Periasamy, H. S. Joo, A. C. Duong, T. H. L. Bach, V. Y.

- Tan, S. S. Chatterjee, G. Y. C. Cheung, M. Otto, *Proc. Natl. Acad. Sci. U. S. A.* **2012**, *109*, 1281–1286.
- [11] K. M. Towle, C. T. Lohans, M. Miskolzie, J. Z. Acedo, M. J. Van Belkum, J. C. Vederas, **2016**, DOI 10.1021/acs.biochem.6b00615.
- [12] S. Satpathy, S. K. Sen, S. Pattanaik, S. Raut, *Biocatal. Agric. Biotechnol.* **2016**, *7*, 56–66.
- [13] K. Schwartz, A. K. Syed, R. E. Stephenson, A. H. Rickard, B. R. Boles, *PLoS Pathog.* **2012**, *8*, DOI 10.1371/journal.ppat.1002744.
- [14] N. Demirdöven, C. M. Cheatum, H. S. Chung, M. Khalil, J. Knoester, A. Tokmakoff, *J. Am. Chem. Soc.* **2004**, *126*, 7981–7990.
- [15] J. P. Lomont, J. S. Ostrander, J.-J. Ho, M. K. Petti, M. T. Zanni, *J. Phys. Chem. B* **2017**, *121*, 8935–8945.
- [16] C. R. Baiz, M. Reppert, A. Tokmakoff, *An Introduction to Protein 2D IR Spectroscopy*, **2013**.
- [17] S. H. Shim, D. B. Strasfeld, Y. L. Ling, M. T. Zanni, *Proc. Natl. Acad. Sci. U. S. A.* **2007**, *104*, 14197–14202.
- [18] S. Woutersen, P. Hamm, *J. Chem. Phys.* **2001**, *115*, 7737–7743.
- [19] M. Grechko, M. T. Zanni, *J. Chem. Phys.* **2012**, *137*, 184202.
- [20] S. H. Lee, S. Krimm, *Chem. Phys.* **1998**, *230*, 277–295.
- [21] A. Barth, C. Zscherp, *Q. Rev. Biophys.* **2002**, *35*, 369–430.
- [22] A. Huerta-Viga, S. Woutersen, *J. Phys. Chem. Lett.* **2013**, *4*, 3397–3401.
- [23] M. R. Panman, C. N. Van Dijk, H. Meuzelaar, S. Woutersen, *J. Chem. Phys.* **2015**, *142*, 41103.
- [24] E. B. Dunkelberger, M. Grechko, M. T. Zanni, *J. Phys. Chem. B* **2015**, *119*, 14065–14075.
- [25] L. P. Deflores, Z. Ganim, R. A. Nicodemus, A. Tokmakoff, *J. Am. Chem. Soc.* **2009**, *131*, 3385–3391.
- [26] M. Khalil, N. Demirdöven, A. Tokmakoff, N. Demirdo, A. Tokmakoff, *J. Phys. Chem. A* **2003**, *107*, 5258–5279.
- [27] A. Ghosh, J. S. Ostrander, M. T. Zanni, *Chem. Rev.* **2017**, *117*, 10726–10759.
- [28] P. Hamm, M. Lim, W. F. Degrado, R. M. Hochstrasser, *The Two-Dimensional IR Nonlinear Spectroscopy of a Cyclic Penta-Peptide in Relation to Its Three-Dimensional Structure*, **1999**.
- [29] C. M. Cheatum, A. Tokmakoff, J. Knoester, *J. Chem. Phys.* **2004**, *120*, 8201–8215.
- [30] Y. S. Kim, R. M. Hochstrasser, *J. Phys. Chem. B* **2009**, *113*, 8231–8251.
- [31] Y. S. Kim, R. M. Hochstrasser, *Proc. Natl. Acad. Sci. U. S. A.* **2005**, *102*, 11185–11190.
- [32] D. Hall, R. Zhao, I. Dehlsen, N. Bloomfield, S. R. Williams, F. Arisaka, Y. Goto, J. A. Carver, *Anal. Biochem.* **2016**, *498*, 78–94.
- [33] O. M. Cracchiolo, D. K. Geremia, S. A. Corcelli, A. L. Serrano, *J. Phys. Chem. B* **2020**, *124*, 6947–6954.
- [34] C. T. Middleton, A. M. Woys, S. S. Mukherjee, M. T. Zanni, *Methods* **2010**, *52*, 12–22.
- [35] A. Ghosh, A. L. Serrano, T. A. Oudenhoven, J. S. Ostrander, E. C. Eklund, A. F. Blair, M. T. Zanni, *Opt. Lett.* **2016**, *41*, 524.
- [36] J. Nishida, A. Tamimi, H. Fei, S. Pullen, S. Ott, S. M. Cohen, M. D. Fayer, *Proc. Natl. Acad. Sci. U. S. A.* **2014**, *111*, 18442–18447.
- [37] C. R. Baiz, D. Schach, A. Tokmakoff, *Opt. Express* **2014**, *22*, 18724.
- [38] M. T. Zanni, N. H. Ge, Yung Sam Kim, R. M. Hochstrasser, *Proc. Natl. Acad. Sci. U. S. A.* **2001**, *98*, 11265–11270.
- [39] P. Hamm, M. Zanni, *Concepts and Methods of 2D Infrared Spectroscopy*, Cambridge University Press, **2011**.
- [40] D. R. Skoff, J. E. Laaser, S. S. Mukherjee, C. T. Middleton, M. T. Zanni, *Chem. Phys.* **2013**, *422*, 8–15.

- [41] V. Cervetto, J. Helbing, J. Bredenbeck, P. Hamm, *J. Chem. Phys.* **2004**, *121*, 5935–5942.
- [42] C. M. Cheatum, A. Tokmakoff, J. Knoester, *J. Chem. Phys.* **2004**, *120*, 8201–8215.
- [43] S. Woutersen, P. Hamm, *J. Chem. Phys.* **2001**, *115*, 7737–7743.
- [44] S. Mukamel, *Principles of Nonlinear Optical Spectroscopy*, Oxford University Press, New York, New York, **1998**.
- [45] D. Abramavicius, S. Mukamel, *Chem. Phys.* **2005**, *318*, 50–70.
- [46] W. Zhuang, D. Abramavicius, T. Hayashi, S. Mukamel, *J. Phys. Chem. B* **2006**, *110*, 3362–3374.
- [47] D. Abramavicius, B. Palmieri, D. V. Voronine, F. Šanda, S. Mukamel, *Chem. Rev.* **2009**, *109*, 2350–2408.
- [48] W. M. Zhang, T. Meier, V. Chemyak, S. Mukamel, *J. Chem. Phys.* **1998**, *108*, 7763–7774.
- [49] H. Torii, M. Tasumi, *J. Chem. Phys.* **1992**, *96*, 3379–3387.

Entry for the Table of Contents



Reporting on the cross- α amyloid forming peptide, Phenol Soluble Modulin alpha3 (PSM α 3), spectroscopic methods reveal cross- α / β polymorphism upon fibrillation. Aggregation studies track PSM α 3 secondary structure elucidating a novel spectroscopic signal unique to cross- α amyloids. Because phenol soluble modulins are an essential component of *Staphylococcus aureus* biofilms, the structural insights gleaned here are relevant to potential therapies.

Supporting Information

Cross- α/β Polymorphism of PSM α 3 Fibrils

Olivia M. Cracchiolo^{[a],[+]}, Dean N. Edun^{[a],[+]}, Vincent M. Betti^[b], Jacob M. Goldberg^[b], and Arnaldo L. Serrano^{*[a]}

[a] Department of Chemistry and Biochemistry, University of Notre Dame
251 Nieuwland Science Hall, Notre Dame, IN 46556
E-mail: arnaldo.serrano@nd.edu

[b] Department of Chemistry, Colgate University
13 Oak Drive, Hamilton, NY 13346
Email: jgoldberg@colgate.edu

[+] These authors contributed equally to this work

[*] Corresponding Author

Table of Contents

Materials and Methods	9
Peptide Synthesis	9
FTIR Spectroscopy	9
2DIR Spectroscopy	9
Narrow-Band Pump Generation	9
Simulation Methods	9
Exciton Scattering Matrix Simulations.....	9
Transmission Electron Microscopy (TEM)	11
Scattered Light Analysis	12
Monomer Spectra	12
Broad Band Pump 2DIR.....	12

Materials and Methods

Peptide Synthesis

Phenol Soluble Modulin alpha-3 (PSM α 3), MEFVAKLFKFFKDLLGKFLGNN-NH₂, was synthesized on a PS3 peptide synthesizer following conventional Fmoc synthesis on a Rink-amide resin. The peptide was cleaved with trifluoroacetic acid (TFA). Following synthesis, the crude peptide was purified on a Jasco LC-4000 HPLC system with a RP-C18 column with molecular weight confirmed by MALDI-MS. The pure peptide was then suspended in hexafluoroisopropanol and 10%(v/v) HCl to exchange TFA. The peptide was then lyophilized overnight and stored as a powder. For IR samples, the dry peptide was suspended in deuterated hexafluoroisopropanol (HFIP-d) to exchange amide hydrogens with deuterium. The sample was left to exchange for 45 minutes. This procedure was repeated twice with the second lyophilization cycle taking place over night to remove any trace solvent.

FTIR Spectroscopy

All FTIR samples were prepared under dry air in a custom sample holder and sandwiched between two 2 mm \times 25.4 mm CaF₂ windows (Crystran Ltd.) with a 50.8 μ m spacer (Scientific Commodities Inc.). Fourier Transform infrared (FTIR) spectra were taken with a Thermo-Nicolet iS50R FTIR spectrometer and detected with an external 1 mm \times 1 mm 20 MHz photovoltaic MCT detector in a sealed box under dry air to prevent inference of atmospheric water.

2DIR Spectroscopy

Details for the 2DIR laser system are described elsewhere.^[1] Briefly, 3.5 mJ, 30 fs, 800 nm pulses from a 1 kHz repetition rate Astrella laser system (Coherent) are directed into a TOPAS prime OPA (Light Conversion) followed by a homebuilt AgGaS₂ based DFG to produce our broadband mid-IR beam. The pump beam is sent through an AOM based mid-IR pulse shaper (PhaseTech Spectroscopy) in order to generate the pulse sequences necessary to perform 2DIR. The waiting time delay between the pump and probe pulses was set to 100 fs. Beam waists were measured to be approximately 30 μ m, using the 80/20 knife-edge method. The probe was directed through the sample into a homebuilt monochromator where the spectrum was detected with a MCT focal plane array camera (Teledyne Catalina). The reference beam spectrum was detected simultaneously on the same camera. Data were processed using custom MATLAB code.

Narrow-Band Pump Generation

To perform the Narrow Band (NB) Pump experiments, we use the capabilities of our AOM to mask all frequencies of the pump beam, leaving only a 3 cm⁻¹ Gaussian window centered at a chosen pump frequency. This window is scanned with 2.7 cm⁻¹ steps in the frequency range from 1600 to 1700 cm⁻¹ to produce the pump axis. The window size and scanning steps were chosen to match the pump resolution of the Broad-Band experiments. Spectra were obtained by scanning line by line along the pump axis, in a manner similar to transient pump-probe collection. We used a [1, off, -1, off] phase cycling scheme to isolate the 2D signal from scattered light. Similar phase combinations of phase cycling have been used for other 2DIR applications.^[2] After fully assembling the 2D spectrum, it was smoothed along the pump axis using a 4 cm⁻¹ Gaussian smoothing window.

Simulation Methods

Exciton Scattering Matrix Simulations

We used the Nonlinear Exciton Scattering Matrix method developed by Mukamel,^[3-5] which avoids the need to diagonalize t_2 -quantum Hamiltonians. Instead, each vibrational mode is treated as a two-state system where the second excited state manifold is accessed through the mixing between excitons calculated through a scattering matrix. The response is then calculated by summing all combinations of four interactions with light. In principle this results in summing up N⁴ interactions, but the complexity

can be greatly reduced by pre-determining all interaction strengths between two excitons and only including scatterings where the interaction strength is greater than a defined threshold. Following Mukamel's implementation^[6] the exciton overlap factor is defined in equation (5).

$$\eta_{e,e'} = \sum_m |\psi_{e,m}| |\psi_{e',m}| \quad (5)$$

We then reject all pairs of interactions where this overlap factor is below 0.55. This number is chosen as it is close to the 0.5 value Mukamel used in demonstrating the effectiveness of the technique while significantly reducing computation time. (For reference, reducing the threshold to 0.5 would effectively double the computation time).

To implement the simulation, first the coordinates for all backbone amide groups in a fibril structure is obtained using coordinates from the crystal structure determined by Landau et al.^[7] Then the one-quantum Hamiltonian is built using the Transition Dipole Coupling model.^[8] We then diagonalize the one-quantum Hamiltonian to obtain the eigen energies and eigenmodes. Pairs of eigenmodes whose exciton overlap are larger than the chosen threshold are retained. The response functions are calculated in the frequency domain using Green's functions. The response for rephasing, $\mathbb{S}_{\nu_4, \nu_3, \nu_2, \nu_1}^{kI}(\Omega_3, t_2, \Omega_1)$, and non-rephasing, $\mathbb{S}_{\nu_4, \nu_3, \nu_2, \nu_1}^{kII}(\Omega_3, t_2, \Omega_1)$ pathways are detailed in the following equations where $\Omega_{1,3}$ and t_2 are the corresponding frequency and time grid points over which the spectrum is calculated. The frequency of each exciton i is ϵ_{e_i} while γ_{e_i} is a phenomenological dephasing rate set to 5cm^{-1} . The $\langle \mu_{e_4}^{\nu_4} \mu_{e_3}^{\nu_3} \mu_{e_2}^{\nu_2} \mu_{e_1}^{\nu_1} \rangle$ term is defined in equation (8) where μ_{e_i} is the transition dipole moment of exciton i and \hat{E}_{ν_i} is a unit vector along the direction of the i^{th} electric field.

$$\begin{aligned} \mathbb{S}_{\nu_4, \nu_3, \nu_2, \nu_1}^{kI}(\Omega_3, t_2, \Omega_1) = & \\ 2i \sum_{e_4 \dots e_1} \langle \mu_{e_4}^{\nu_4} \mu_{e_3}^{\nu_3} \mu_{e_2}^{\nu_2} \mu_{e_1}^{\nu_1} \rangle \times & I_{e_1}^*(t_2) I_{e_2}(t_2) \mathfrak{I}_{e_1}^*(-\Omega_1) \mathfrak{I}_{e_4}(\Omega_3) \times \Gamma_{e_4 e_1, e_3 e_2}^{ex}(\Omega_3 + \epsilon_{e_1} \\ & + i\gamma_{e_1}) \mathcal{J}_{e_3 e_2}(\Omega_3 + \epsilon_{e_1} + i\gamma_{e_1}) \end{aligned} \quad (6)$$

$$\begin{aligned} \mathbb{S}_{\nu_4, \nu_3, \nu_2, \nu_1}^{kII}(\Omega_3, t_2, \Omega_1) = & \\ 2i \sum_{e_4 \dots e_1} \langle \mu_{e_4}^{\nu_4} \mu_{e_3}^{\nu_3} \mu_{e_2}^{\nu_2} \mu_{e_1}^{\nu_1} \rangle \times & I_{e_1}(t_2) I_{e_2}^*(t_2) \mathfrak{I}_{e_1}(\Omega_1) \mathfrak{I}_{e_4}(\Omega_3) \times \Gamma_{e_4 e_2, e_3 e_1}^{ex}(\Omega_3 + \epsilon_{e_2} \\ & + i\gamma_{e_2}) \mathcal{J}_{e_3 e_1}(\Omega_3 + \epsilon_{e_2} + i\gamma_{e_2}) \end{aligned} \quad (7)$$

$$M_{e_4 e_3 e_2 e_1}^{\nu_4 \nu_3 \nu_2 \nu_1} \equiv \langle (\mu_{e_4} \cdot \hat{E}_{\nu_4}) (\mu_{e_3} \cdot \hat{E}_{\nu_3}) (\mu_{e_2} \cdot \hat{E}_{\nu_2}) (\mu_{e_1} \cdot \hat{E}_{\nu_1}) \rangle \quad (8)$$

Where $I_{e'}$, $\mathfrak{I}_{e'}$, and $\mathcal{J}_{e'e''}$ are defined as:

$$I_{e'}(t) = \theta(t) \exp(-i\epsilon_{e'}t - \gamma_{e'}t) \quad (9)$$

Where $\theta(t)$ is the Heaviside function.

$$\mathfrak{I}_{e'}(\omega) = \frac{i}{\omega - \epsilon_{e'} + i\gamma_{e'}} \quad (10)$$

$$\mathcal{J}_{e'e''}(\omega) = \frac{i}{\omega - \epsilon_{e'} - \epsilon_{e''} + i(\gamma_{e'} + \gamma_{e''})} \quad (11)$$

The gamma terms are defined below.

$$\Gamma_{e_4 e_1, e_3 e_2}^{ex}(\omega) = \sum_{m,n} \psi_{e_4 m}^* \psi_{e_1 m}^* \Gamma_{m,n}^{site} \psi_{e_3 n} \psi_{e_2 n} \quad (12)$$

$$\Gamma_{m,n}^{site}(\omega) = -i \bar{\Delta}_m (\bar{D}^{-1})_{m,n} \quad (13)$$

Where $\bar{D}_{m,n}$ is

$$\bar{D}_{m,n} = \delta_{mn} + i \mathcal{G}_{m,n} \bar{\Delta}_n \quad (14)$$

Finally, the Green function, $\mathcal{G}_{m,n}(\omega)$ is as follows.

$$\mathcal{G}_{m,n}(\omega) = \sum_{e',e''} \psi_{e' m} \psi_{e'' m} \mathcal{J}_{e'e''}(\omega) \psi_{e' n}^* \psi_{e'' n}^* \quad (15)$$

Transmission Electron Microscopy (TEM)

Upon incubation the sample was centrifuged at 14,800 rpm for 20 minutes. The supernatant was decanted off and the pellet was resuspended in a 10-fold dilution following the protocol from Landau et al.^[9,10] 5 mL of sample was then adhered to a 400-mesh copper TEM grid with Formvar/Carbon support films (Ted Pella, distributed by Getter Group Bio Med, Petah-Tikva, Israel), that had been glow discharged and stained with 2% uranyl acetate. The sample was imaged at 20 keV with 100 nm resolution.

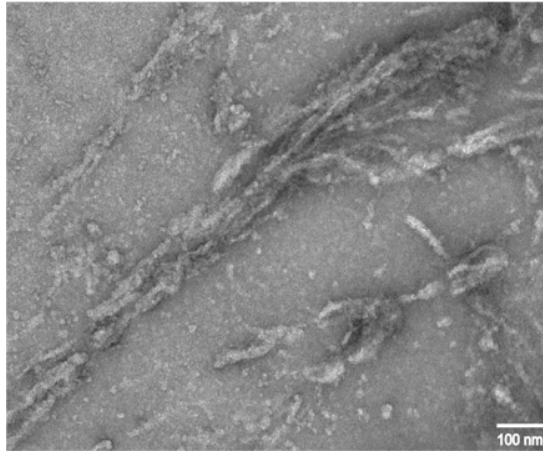


Figure S1. Transmission electron microscopy image of PSM α 3 fibrils formed after room temperature incubation. Scale bar indicates 100 nm.

Scattered Light Analysis

To ensure the spectra obtained correspond to fibrils in the sample, a scattering analysis was performed using the time domain data. An alternative phase cycling scheme (given in equation 3 of the main text) was used to maximize scattered light interference signals, which are used as an in-situ measure of the presence of aggregates. The sample in Figure S2a corresponds to the monomeric solution and therefore the scattered light is negligible, while the samples in Figures S2 b and c contain fibers, resulting in intense scattered light.

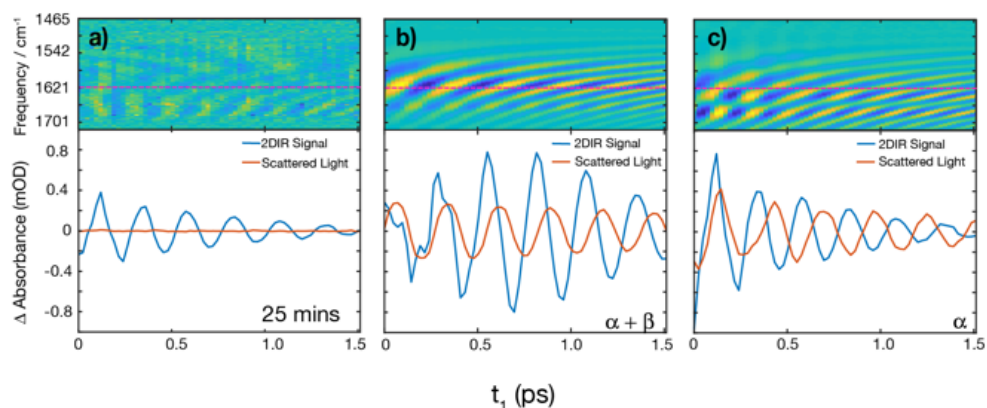


Figure S2. 2DIR signal compared to scattered light. The time domain data for scattered light is depicted in the top panels. The bottom plots show the 2DIR signal (blue) and scattered light (orange) along the horizontal slices (pink dashed line) taken at 1621 cm^{-1} of a PSM α 3 solution after 25 mins, b) the $\alpha + \beta$ fibrils and c) the isolated cross- α fibril.

Monomer Spectra

Broad Band Pump 2DIR

The BB experiments were performed with 0.5 mM PSM α 3 to capture the spectra of the monomer.

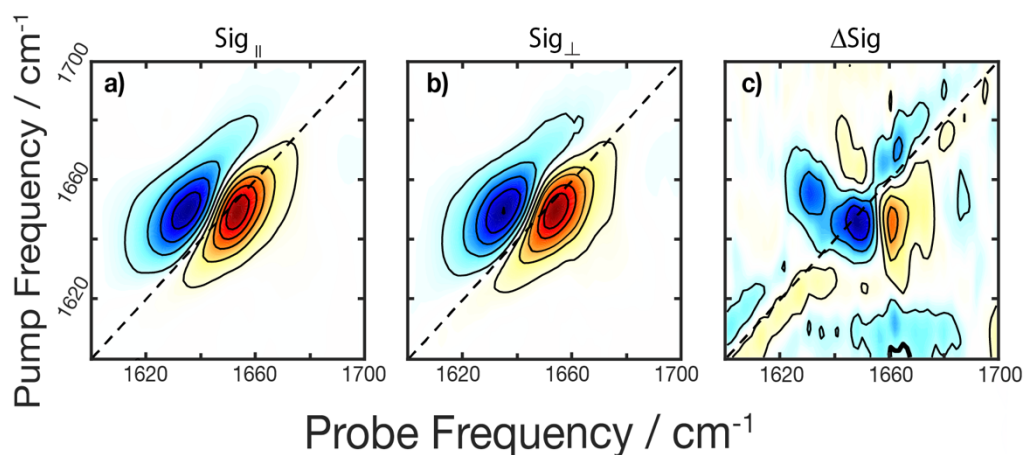


Figure S3. BB 2DIR spectrum of 0.5 mM PSM α 3 in D₂O taken with a) parallel b) and perpendicular polarizations using broad band pump. The difference spectrum is shown in c).

The experimental and simulated difference spectra shown side by side in Figure S5 reveal a similar peak pattern. The simulated spectrum captures the same spectral features observed experimentally.

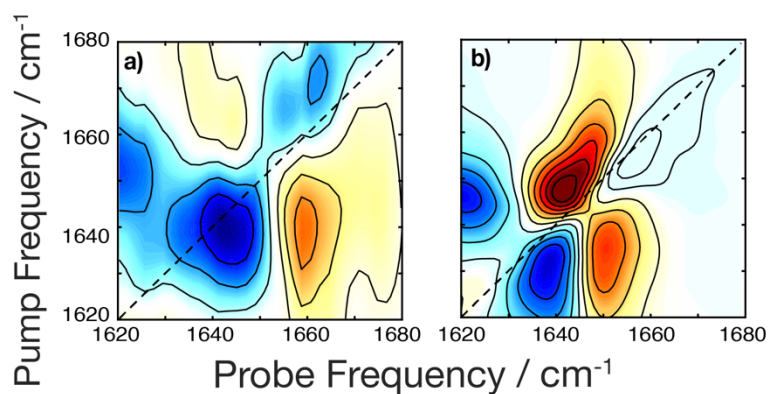


Figure S4. BB 2DIR difference spectrum of a) 0.5 mM PSM α 3 in D₂O b) simulated monomer difference spectrum

References

- [1] O. M. Cracchiolo, D. K. Geremia, S. A. Corcelli, A. L. Serrano, *J. Phys. Chem. B* **2020**, *124*, 6947–6954.
- [2] C. R. Baiz, D. Schach, A. Tokmakoff, *Opt. Express* **2014**, *22*, 18724.
- [3] S. Mukamel, *Principles of Nonlinear Optical Spectroscopy*, Oxford University Press, New York, New York, **1998**.
- [4] D. Abramavicius, B. Palmieri, D. V. Voronine, F. Šanda, S. Mukamel, *Chem. Rev.* **2009**, *109*, 2350–2408.
- [5] W. Zhuang, D. Abramavicius, T. Hayashi, S. Mukamel, *J. Phys. Chem. B* **2006**, *110*, 3362–3374.
- [6] W. M. Zhang, T. Meier, V. Chemyak, S. Mukamel, *J. Chem. Phys.* **1998**, *108*, 7763–7774.
- [7] N. Salinas, J. P. Colletier, A. Moshe, M. Landau, *Nat. Commun.* **2018**, *9*, 3512.
- [8] H. Torii, M. Tasumi, *J. Chem. Phys.* **1992**, *96*, 3379–3387.
- [9] E. Tayeb-Fligelman, O. Tabachnikov, A. Moshe, O. Goldshmidt-Tran, M. R. Sawaya, N. Coquelle, J. P. Colletier, M. Landau, *Science (80)*. **2017**, *355*, 831–833.
- [10] E. Tayeb-Fligelman, N. Salinas, O. Tabachnikov, M. Landau, *Structure* **2020**, *28*, 301-313.e6.